

# Thermodynamics of P<sub>2</sub>O<sub>5</sub>-Containing Slag and the Gas-Slag Equilibrium in the Waste Melting Process

Chunlin Chen<sup>1)</sup> T. Tsunemi<sup>2)</sup> T. Kitamura<sup>2)</sup> H. Ohtani<sup>3)</sup> M. Tokuda<sup>1)</sup>

1) Center for Northeast Asian Studies, Tohoku University, Sendai, Japan

2) Research Center, Osaka Gas Co., Ltd. Osaka, Japan

3) Center for Interdisciplinary Research, Tohoku University, Sendai, Japan

**ABSTRACT** The parameters of Na<sub>2</sub>O-P<sub>2</sub>O<sub>5</sub> and Na<sub>2</sub>O-SiO<sub>2</sub> systems used in the cell model have been assessed. The cell model was used to calculate the activities of components in the slag phase, and the gas phase was treated as ideal in simulations of the waste melting process. The calculated slag and gas compositions were compared with plant data and satisfactory agreement was obtained. The calculated results show that 73% P in charged materials entered the gas phase and were later deposited out on the wall of the waste heat boiler as H<sub>3</sub>PO<sub>4</sub>, contributing to the corrosion observed there. The addition of CaO to the process was found to promote fixation of P in the slag phase, thus reducing the corrosion of the waste heat boiler.

## 1 Introduction

In recent years, the awareness of the necessity to preserve the environment and to conserve our limited natural resources has led to increasingly strict requirements for recycling wastes. The waste melting process described in this paper is a type of process which enables a considerable reduction of volume, stabilization and utilization of sewage sludge<sup>[1]</sup>. In this process, dewatered sludge cake, coke and flux are charged into the melting furnace where the combustibles contained in the sludge are burned on the coke bed. Non-combustibles are melted down and recovered in the form of non-hazardous slag which is safely used as road paving material and building material. The gas-slag reactions are of considerable industrial interest. An understanding of these reactions can help us to predict and control the distribution of elements and then to optimize the industrial operations. In this work, the waste melting process was simulated through the multi-components and multi-phases equilibrium method. The calculated results on slag and gas compositions are compared with plant data.

## 2 Industrial Trial

An industrial trial of the process was carried out in sludge treatment plant A in 1998. The charged materials as well as products such as sludge cake, blowing air, exhaust gas and dust were sampled and then chemically analyzed. The input rate of charged materials and the temperature of gas were also recorded. The compositions and input rates of the charged materials are listed in Table 1<sup>[2]</sup>.

## 3 Simulation System

The complexity of the industrial process generally necessitates that a number of assumptions be made in order to simplify the modeling process. The most important assumption is that the melting system is in both chemical and thermal equilibrium. In this case, it is assumed that all the charged materials during a given time step are in equilibrium. In the industrial furnace, the temperature is unevenly distributed. In order to simulate the process accurately and simply, the furnace was divided into three reaction zones. These zones were simulated sequentially. The melting furnace is illustrated in Fig.1. The system is assumed to consist of a gas phase, a

slag phase and condensed phases. According to the analytic results of industrial charged materials, the system contains 16 elements, namely, Pb, Zn, Al, Ca, Fe, Mg, P, K, Na, Si, C, S, Mn, H, N and O, and the components of each phase are assumed to be as follows:

Gas phase:  $N_2$ ,  $NH_3$ ,  $CH_4$ ,  $S_2$ ,  $ZnS$ ,  $CS$ ,  $CS_2$ ,  $SO$ ,  $SO_2$ ,  $CO$ ,  $CO_2$ ,  $SO_3$ ,  $Zn$ ,  $H_2S$ ,  $H_2$ ,  $HS$ ,  $H_2O$ ,  $MnO$ ,  $Na$ ,  $MgO$ ,  $Na_2O$ ,  $Mg$ ,  $NO_2$ ,  $N_2O_5$ ,  $K$ ,  $K_2O$ ,  $FeS$ ,  $P_4O_{10}$ ,  $CaH$ ,  $KH$ ,  $NaH$ ,  $Na_2SO_4$ ,  $K_2SO_4$ ,  $P_4$ ,  $SiO$ ,  $PN$ ,  $SN$ ,  $KCN$ ,  $NaCN$ ,  $CN$ ,  $COS$ ,  $K_2(CN)_2$ ,  $C_2N_2$  and  $P_4S_3$

Slag phase:  $Al_2O_3$ ,  $SiO_2$ ,  $P_2O_5$ ,  $CaO$ ,  $FeO$ ,  $Fe_2O_3$ ,  $Na_2O$ ,  $MgO$ ,  $MnO$ ,  $K_2O$  and  $ZnO$

Condensed phase:  $Na_2CO_3$ ,  $Na_2SO_4$ ,  $Na_2SO_3$ ,  $K_2SO_4$ ,  $K_2SO_3$ ,  $KH_2PO_4$ ,  $H_3PO_4$ ,  $ZnS$ ,  $ZnO$ ,  $ZnSO_4$ ,  $SiO_2$ ,  $Al_2O_3$ ,  $Na_4P_2O_7$ ,  $CaCO_3$ ,  $FeO$ ,  $Fe_2O_3$ ,  $SiO_2$ ,  $Ca_3P_2O_8$ ,  $Ca_2P_2O_7$ ,  $K_2CO_3$ ,  $Zn$ ,  $FeS$ ,  $MgS$ ,  $CaS$ ,  $Al_2S_3$ ,  $Na_2S$ ,  $C$ ,  $S$ ,  $Fe_3C$ ,  $P$ ,  $CaC_2$ ,  $Al_4C_3$ ,  $Mg_3P_2O_8$ ,  $MgC_2$ ,  $SiC$  and  $K_2S$

During the calculation, the gas phase can be treated as ideal while the molten slag phase is not so. In thermodynamic studies, it is important to choose an appropriate solution model to calculate the activities of components in the slag phase. As listed above, the molten slag phase is a mixture of oxides. Among the models concerning slag, the cell model and the modified quasi-chemical model are now widely used in the calculation of oxide slag<sup>[3-6]</sup>. These two models are all extended to poly-anionic and multi-component systems. The parameters which will be used in the modified quasi-chemical model of all binary subsystems in 11 components, namely,  $Si_2O$ - $CaO$ - $Al_2O_3$ - $FeO$ - $MgO$ - $MnO$ - $Na_2O$ - $K_2O$ - $TiO_2$ - $Ti_2O_3$ - $Zr_2O$ - $S$ , have been evaluated<sup>[7]</sup>. The cell model parameters for the  $P_2O_5$ - $SiO_2$ - $Cr_2O_3$ - $Al_2O_3$ - $Fe_2O_3$ - $CrO$ - $FeO$ - $MnO$ - $MgO$ - $CaO$  system have been assessed by Gaye *et.al*<sup>[8]</sup>. According to the industrial report, the content of P in slag is about 2 wt%, so  $P_2O_5$  should be considered in the slag system. In the present work, the cell model was chosen to calculate the activities of components in sludge melting slag.

#### 4 Assessment of the Parameters Used in the Cell Model

Cell model uses two kinds of energy parameters to describe the formation of cells ( $W_{ij}$ ) and the interaction between cells ( $E_{ij}$ ) and give an expression for activity coefficient in liquid slags as a function of temperature and composition.

##### *Systems Containing $Na_2O$*

$Na_2O$  is included in the slag system. The parameters of the  $Na_2O$ - $P_2O_5$  system used in the cell model are still lacking. In order to simulate the process precisely and to study the influence of  $Na_2O$  on the behavior of  $P_2O_5$  in slag, the parameters of  $Na_2O$ - $P_2O_5$  have been optimized:  $W_{NaP} = -132$  KJ,  $E_{NaP} = -165$  KJ. Due to the high content of  $SiO_2$  in the slag phase, the effect of  $SiO_2$  on  $Na_2O$  is prominent. Adding the parameters of the  $Na_2O$ - $SiO_2$  system to the model will make the simulated results become closer to the practical ones. Through the assessment, the following parameters are obtained:  $W_{NaSi} = -92$  KJ,  $E_{NaSi} = 45$  KJ. The validity of the assessment is illustrated in Fig. 2 and Fig. 3, respectively. As shown in Figs. 2 and 3, the general agreement between model prediction and experimental values is rather good.

##### *Activity Coefficient of $K_2O$ in Slag*

The measured activity data for the  $K_2O$  binary system are not available so far. This makes it impossible to optimize the model parameters between  $K_2O$  and other species and to incorporate  $K_2O$  in a non-ideal solution model. Turkdogan derived the activity of  $K_2O$  in the  $K_2O$ - $CaO$ - $MgO$ - $SiO_2$ - $Al_2O_3$  slag system. The following coefficient-composition relationship for  $K_2O$  was derived from Turkdogan's results by H.-J. Li et al.<sup>[9]</sup>

$$\gamma_{K_2O} = 2.86 \times 10^{-10} (\text{wt pct } K_2O)^2 / X_{K_2O} \quad (1)$$

The gas-slag equilibrium in the sludge melting furnace was calculated by using a commercial software package-ChemSage, incorporating the cell model for the slag phase and the empirical expression (1) for  $K_2O$ .

## 5 Results and Discussion

As mentioned previously, the melting furnace was divided into three parts which were simulated sequentially.

### *The First Reaction Zone*

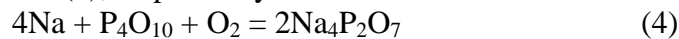
Due to the high temperature in the furnace and the charge of the sludge cake from the upper part of the furnace, all of the water in the cake is assumed to have already evaporated and reacted with other reactants in the second zone before the cake reached the coke bed. The sludge ash was combusted and melted down to form the slag on the coke bed. The calculated compositions of the slag and gas phase in this zone with the relevant plant data are listed in Tables 2 and 3, respectively. The comparisons show that the calculated contents of elements in the slag are in good agreement with those of the plant data. It's very difficult to sample the gas in this zone during the melting process. For this reason, the calculated composition of the gas phase can't be directly compared with the relevant plant data. The calculated results show that the main components of gas are  $N_2$ ,  $H_2$  and  $CO$ . Because the first zone is under strong reduction conditions, most of P in gas is assumed to exist as a form of PN which might be formed through the following two reactions.



The distribution of phosphorus among components is shown in Table3. The amount of  $P_4O_6$  in gas is small. The condensed phase didn't appear in this step from the viewpoint of thermodynamic calculation.

### *The Second Reaction Zone*

The water vaporized from the cake, air 23 and the gas from the first zone mixed together and reacted in the second reaction zone at a temperature of about 1373 K. The calculated gas and dust compositions are shown in Tables 4 and 5, respectively. Due to the input of air 23,  $H_2O$  and  $CO_2$  are calculated to appear predominantly in the gas phase instead of  $H_2$  and  $CO$  in the first zone. PN was also oxidized to  $P_4O_{10}$ . Excessive oxygen in the gas is about 2.2 Vol%. The Na and SiO in the gas phase deposited out as a form of  $Na_4P_2O_7$  and  $SiO_2$  dust at the same time by reaction (4) and reaction (5), respectively.



### *The Third Reaction Zone*

All of the gas and dust from the second zone are assumed to be the reactants in the third zone. Boiler tubes were inserted in the upper portion of the furnace to absorb waste heat. The temperature in this zone was controlled at about 1063K by introducing cooled gas into the furnace. The calculated equilibrium composition of the gas and condensed phase are listed in Tables 6 and 7, respectively. Zn and  $K_2SO_4$  in the gas from the second zone were deposited out as  $ZnSO_4$  and  $K_2SO_4$ . It is clear that the main components such as  $CO_2$ ,  $O_2$ ,  $H_2O$  and  $N_2$  in the gas phase agree with the measured data.

As the exhaust gas coming out of the furnace is very hot, the heat was recovered by an air pre-heater and a waste heat boiler. The temperature of the exhaust gas was decreased to 943 K and 473 K, in the pre-heater and boiler, respectively. Thermodynamic simulation of conditions in the air pre-heater and the waste heat boiler was also carried out. The results show that although there is no deposition at the temperature of air pre-heater, nearly all of the

P in the exhaust gas was deposited out as  $\text{H}_3\text{PO}_4$  at 473 K through reaction (6) on the wall of the waste heat boiler, contributing to the corrosion observed there.



#### *Effects of CaO on the Distributions of P in the Melting System*

It is well known that high basicity of slag can improve the phosphorus capacity in the slag. According to the interaction parameter of  $\text{Ca}^{2+}$  and  $\text{P}^{5+}$  which was assessed by Gaye<sup>[4]</sup>, the formation energy of Ca-O-P is -73.59 KJ. It is clear that the Ca-O-P pair is easily formed. The addition of CaO helps decrease the activity coefficient of  $\text{P}_2\text{O}_5$  in slag. Although the formation energy of Na-O-P, which was assessed as being -165 KJ by the author is more negative than that of Ca-O-P, the use of  $\text{Na}_2\text{O}$  causes considerable difficulty in practice due to the erosion of refractories and the evaporation of  $\text{Na}_2\text{O}$ . The melting process was simulated under the situation of charging different amounts of CaO into the furnace. The calculated results are shown in Fig. 4. The P increases in slag with increasing CaO content, as expected. When the basicity of slag increases to 1.3, nearly 50% P enters the slag phase. The addition of CaO to the process was found to be an effective way to fix more phosphorus in the slag, which alleviates the corrosion of the waste heat boiler by  $\text{H}_3\text{PO}_4$ .

## 6 Conclusion

The parameters of  $\text{Na}_2\text{O}$ - $\text{P}_2\text{O}_5$  and  $\text{Na}_2\text{O}$ - $\text{SiO}_2$  systems which were used in the cell model have been assessed. These parameters, combined with other published cell model parameters and the empirical expression of the activity coefficient of  $\text{K}_2\text{O}$ , were used in the cell model to calculate activities for species in the sludge melting slag while the gas was treated as ideal. The calculated compositions of slag and exhaust gas from the melting furnace show good agreement with the plant data. This also means that simulating the sludge melting process through the multi-component and multi-phase equilibrium method is reasonable and effective. From the simulation results, it is clear that nearly 27% P enters the slag phase. The remainder, that was in the gas phase, will be deposited later in the form of  $\text{H}_3\text{PO}_4$  in the waste heat boiler. P that precipitates on the wall of the waste heat boiler as  $\text{H}_3\text{PO}_4$  contributes to the corrosion observed there.

The addition of more CaO to the process was found to promote fixation of P in the slag phase, resulting in a reduction of the corrosion of the waste heat boiler.

## Reference

- [1] N. Takeda, M. Hiraoka, S. Sakai, K. Kitai and T. Tsunemi: *Wat. Sci. Tech. Vol.21*, 989:925
- [2] Industrial test reports of the waste melting process, Osaka Gas Copr., 1998
- [3] H-J. Li and M. Tokuda: *Steel Research*, 1993 Vol 93(1): 39
- [4] H-J. Li and M. Tokuda: *ISIJ International*, 1993, Vol 33(5): 539
- [5] H.-J.Li, H. Suito and M. Tokuda: *The Iron and Steel Institute of Japan*, 1995, Vol 35(9):1079
- [6] S.Osada, H.Ono, M.Osada, M. Kokado and M.Tokuda: *The Second International Conference on EcoBalance*, 1996, Tsukuba: P537
- [7] A.D. Pelton and M. Blander: *Metall. Trans. B*, 1986, Vol 17B:805
- [8] H.Gaye, J. Lehmann, T. Matsumiya and W. Yamada: *Proc. 4<sup>th</sup> Int. Conf. On Molten Slags and Fluxes, ISIJ, Sendai, Japan, 1992: 103*
- [9] H.-J. Li, A. E. Morris and D. G. C. Robertson: *Matall. And Metal. Trans. B*, 1998, Vol 29B: 1181

- [10] S. Yamaguchi and K.S.Goto: *J. Jpn. Inst. Met.*, 1984, Vol 48: 43  
 [11] F. Tsukihashi, F. Matsumoto, T. Hyodo, M. Yukinobu and N. Sano: *Tetsu-to-Hagane*, 1985, Vol 71: 815

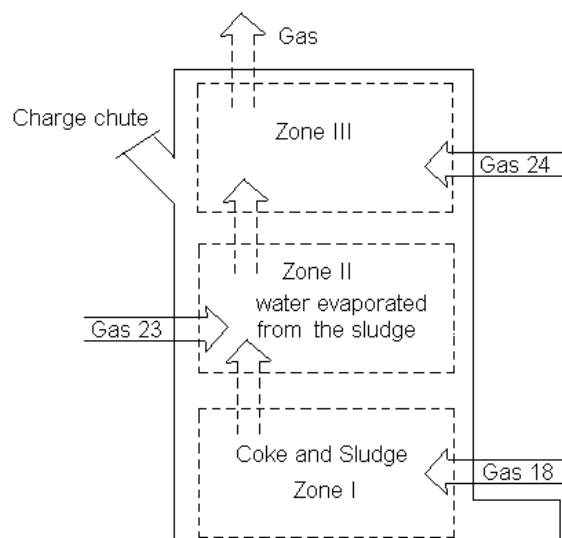


Fig. 1 Schematic diagram of melting process

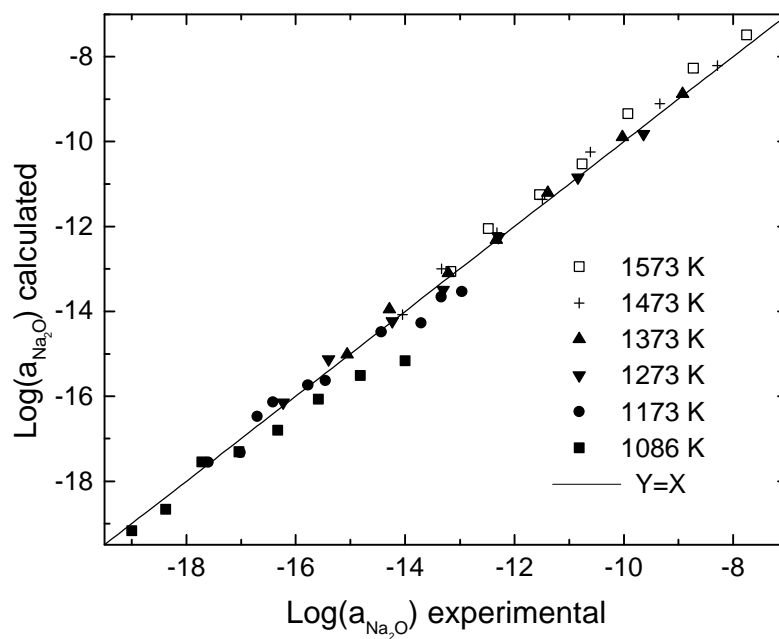


Fig. 2 Comparison of experimental and calculated  $\text{Na}_2\text{O}$  activity in the system  $\text{Na}_2\text{O-P}_2\text{O}_5$ <sup>[10]</sup>

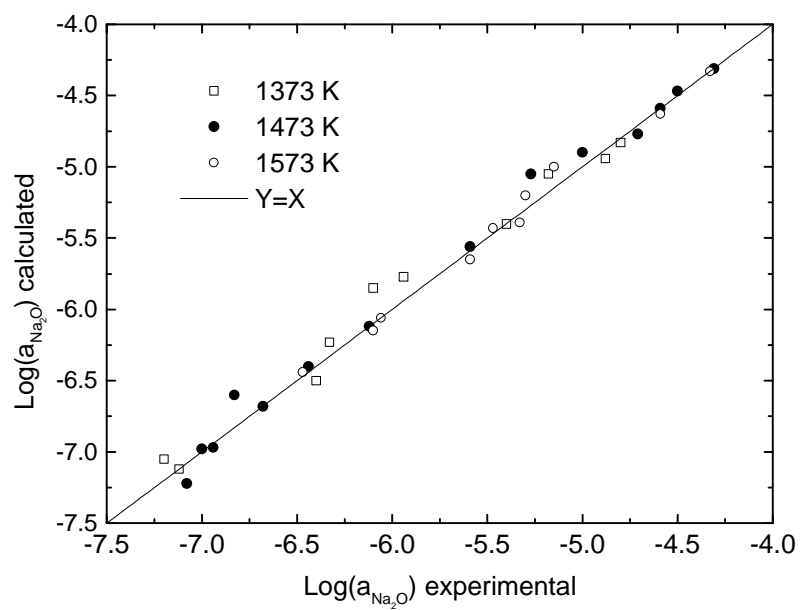


Fig. 3 Comparison of experimental and calculated  $\text{Na}_2\text{O}$  activity in the system  $\text{Na}_2\text{O-SiO}_2$ <sup>[11]</sup>

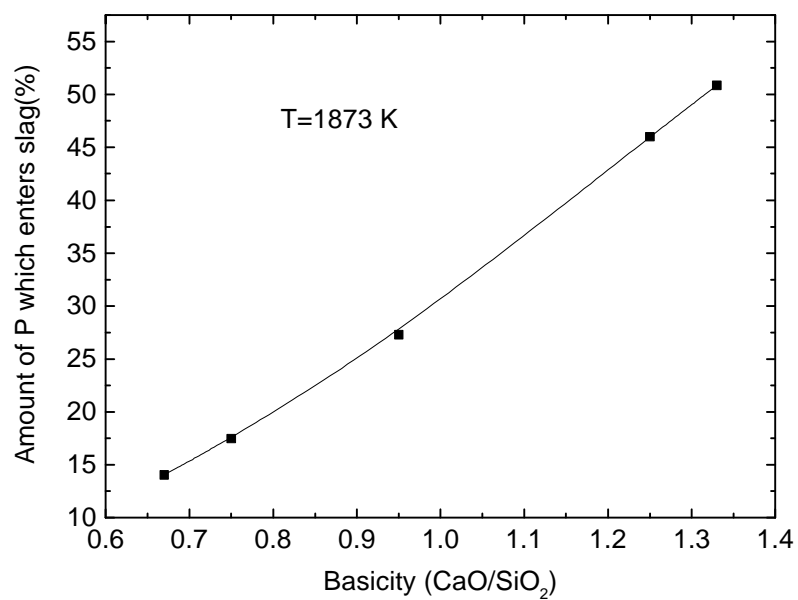


Fig. 4 Effect of CaO on the distribution of P in slag

**Table 1. Compound compositions in charged materials**

	Input gas 18	Input Gas 23	Input Gas 24	Lime Stone	Cake	Coke
Unit	mol/min	mol/min	mol/min	mol/min	mol/min	mol/min
Pb	0	0	0	0	0.0006	0
Zn	0	0	0	0	0.19	0
Al	0	0	0	0.018	7.84	5.48
Ca	0	0	0	7.82	0.16	0.16
Fe	0	0	0	0.01	2.64	0.75
Mg	0	0	0	0.18	1.55	0.097
Mn	0	0	0	0	0.06	0
P	0	0	0	0	6.30	0.082
K	0	0	0	0	1.44	0.2
Na	0	0	0	0	0.84	0
Si	0	0	0	0.07	19.98	8.18
C	0	0	0	0	258.6	326.6
S	0	0	0	0	1.36	0.06
O <sub>2</sub>	286	401	81	0	0	0
N <sub>2</sub>	1075	1510	304.83	0	0	0
H <sub>2</sub> O	36	106	10.33	0	372.2	7.5

**Table 2. Comparison between the calculated and the measured results of the slag phase**

	Al	Ca	Fe	Mg	Mn	K	Na	Si	P
Unit	Wt%	Wt%	Wt%	Wt%	Wt%	Wt%	Wt%	Wt%	Wt%
Measured Data	7.94	25.23	1.22	1.55	0.09	1.21	0.44	15.90	1.92
Calculated Data	8.85	24.02	4.64	1.21	0.08	1.50	0.46	16.63	1.34

**Table 3. Calculated composition of the gas phase in Zone I**

	H <sub>2</sub> O Vol%	N <sub>2</sub> Vol%	H <sub>2</sub> Vol%	CO <sub>2</sub> Vol%	CO Vol%	PN Vol%
Calculated Data	0.17	61.79	1.89	0.73	33.86	0.21

**Table 4. Calculated composition of the gas phase in Zone II**

	H <sub>2</sub> O Vol%	N <sub>2</sub> Vol%	O <sub>2</sub> Vol%	CO <sub>2</sub> Vol%	P <sub>4</sub> O <sub>10</sub> Vol%
Calculated Data	13.45	67.60	2.23	15.38	0.03

**Table 5. Calculated composition of the dust in Zone II**

	Na <sub>4</sub> P <sub>2</sub> O <sub>7</sub> Mol/min	SiO <sub>2</sub> Mol/min
Calculated Data	0.0045	0.026

**Table 6. Comparison between the calculated and the measured results of gas phase in Zone III**

	H <sub>2</sub> O	N <sub>2</sub> Vol%	O <sub>2</sub> Vol%	CO <sub>2</sub> Vol%	P <sub>4</sub> O <sub>10</sub> Vol%
Calculated Data	12.39	68.47	3.92	13.88	0.027
Measured Data	15.9	68.0	2.9	13.1	

**Table 7. Calculated composition of the dust in Zone III**

	K g/min	Na g/min	Si g/min	Zn g/min	P g/min
Calculated Data	2.89	0.42	0.74	12.32	0.28